Electrokinetics in Earth Sciences: A Tutorial

Laurence Jouniaux, Tsuneo Ishido

Hindawi Publishing Corporation
International Journal of Geophysics
Volume 2012, Article ID 286107, 16 pages
doi:10.1155/2012/286107

Review Article

Electrokinetics in Earth Sciences: A Tutorial

L. Jouniaux[1] and T. Ishido[2]

[1] *Institut de Physique du Globe de Strasbourg, UdS-CNRS UMR 7516, Université de Strasbourg, 5 rue René Descartes, 67084 Strasbourg, France*
[2] *Geological Survey of Japan, National Institute of Advanced Industrial Science and Technology (AIST), Tsukuba, Ibaraki 305-8567, Japan*

Correspondence should be addressed to L. Jouniaux, laurence.jouniaux@unistra.fr

Received 1 June 2011; Accepted 14 October 2011

Academic Editor: Rudolf A. Treumann

We describe in this paper the theoretical background for the electrokinetics in rocks and in porous media, to be included in the special issue "Electrokinetics in Earth Sciences" of International Journal of Geophysics. We describe the methodology used for self-potential (SP) and for seismoelectromagnetic measurements, for both field and laboratory experiments and for modelling. We give a large bibliography on the studies performed in hydrology to detect at distance the water flow, to deduce the thickness of the aquifer and to predict the hydraulic conductivity. The observation of SP has also been proposed to detect fractures in boreholes, to follow the hydraulic fracturing, and to predict the earthquakes. Moreover, we detail the studies on geothermal applications.

1. Introduction

The electrokinetic phenomena are induced by the relative motion between the fluid and the rock matrix. In a porous medium, the electric current density, linked to the ions within the fluid, is coupled to the fluid flow [1] so that the streaming potentials are generated by fluids moving through porous media [2].

The SP method consists in measuring the natural electric field on the earth's surface. Usually, the electric field is measured by a high-input impedance multimeter, using impolarizable electrodes [3, 4], and its interpretation needs filtering techniques [5]. Moreover, for long-term observations, the monitoring of the magnetic field is also needed for a good interpretation [6]. The classical interpretation of the self-potential (SP) observations is that they originate from electrokinetic effect as water flows through aquifer or fractures. Surface observations of SP anomalies have been reported from numerous tectonically active areas in the world, at different scales from centimetric to kilometric, at the earth surface or in boreholes.

The SP method has been used to characterize active volcanic areas, usually showing positive anomalous electric signals [7–13]. These anomalous signals are commonly attributed to electrokinetic processes induced by upward hydrothermal flow. The SP sources have been localized at depth using multiscale wavelet tomography [14, 15]. However, numerical modeling showed that these SP anomalies can be induced by meteoric flow in the nonsaturated zone and are linked to the spatial distribution of the electrical conductivity [16–18]. Moreover, a recent study showed that air convection can also be present if the porous medium is highly permeable [19], leading to the conclusion that the effect of water-content on the electrokinetic processes should be better known [20–24].

Monitoring the SP has been proposed as a possible means for predicting earthquakes [25, 26]. Indeed, the electrokinetic effects may be produced by fluid percolation in the crust, driven by a pore pressure gradient related to precursory deformation [25]. In this case, dilatancy prior to the earthquake [27, 28] is assumed to enhance the permeability of the medium and allows the fluid to flow in the vicinity of the fault [29]. It has also been proposed a long-distance elastic effect near the electrodes of measurement [30]. Bernard [31] proposed an electrokinetic model based on the triggering of fluid instabilities at the measurement site responding nonlinearly to precursory strain. However, the long-distance effects are still controversial, as their

observation requires the coincidence of very favorable circumstances to take into account a reasonable precursory strain and the fact that no coseismic electrical anomalies are observed. Another interpretation was proposed on the basis of laboratory observations showing that the electrokinetic coupling of a rock was enhanced by fracturing [32, 33], when stresses rise to over 75% of the yield stress that ruptures the seismic zone. Moreover, the oscillatory nature of some observations has been attributed to an electrokinetic effect associated with unsteady fluid flow during failure of faults. Fenoglio et al. [34] suggested that the stop-and-go fracture propagation associated with rapid fluid flow in a shear fracture 17 km deep could generate electric and magnetic signals measurable at the surface as a result of electrokinetic effects.

Some anomalous electric signals were interpreted as due to the change of the self-potential of the fractured fault rock in which one electrode was fixed, the other electrode being at a constant potential serving as a reference [35]. The detection of fractures and cracks is possible through streaming potential response to a pressure pulse in a borehole [36]. The propagation of hydraulic fracturing could also be detected at distant by measuring the electrical field. The hydraulic fracturing can induce streaming potentials as the fracture propagates, if the fracture remains fulfilled with water. Laboratory experiments on hydraulic fracturing on granite samples showed that the streaming potential varies linearly with the injection of pressure, with an exponential trend when approaching the breakdown pressure [37]. The modeling of the streaming potential induced by an advancing crack showed that the streaming electric current is maximum at the tip of the fracture and decays exponentially in front of the tip [38]. Hydraulic stimulation is often used to stimulate fluid flow in geothermal reservoirs, and surface electrical potential has been monitored around geothermal wells [39]. An anomalous potential of about 5 mV at the Soultz Hot Dry Rock site (France) was interpreted as an electrokinetic effect at 5 km depth and measured at the surface because of the conductive well casing [40]. The SP anomaly was essentially related to water-flows after the earliest stage of injection [41–44]. The observed SP decay after shut-in was interpreted as related to large fluid-flow persisting after the end of stimulation and correlated to the microseismic activity [45]. Another field experiment was performed with periodic pumping tests (injection/production) and showed that the attenuation of SP amplitude with distance was roughly similar to the pressure attenuation [46], leading to the conclusion that the hydraulic diffusivity could be inferred from SP observations.

The distribution of SP can be used to map ground water flow features. Time-varying fluid flow has been identified through SP measurements, showing clearly both rainfall and evaporation events [47]. Modelling of such observations confirmed that SP measurements allow effectively to estimate the direction of water flux at the scale of the electrode separation (usually several decimetres), that is, at a much larger scale than tensiometric measurements [41]. It has been proposed to use SP observations to infer water-table variations and some observations of SP can yield an estimate of aquifer hydraulic properties. It has been proposed to deduce not only the equivalent electric sources, but also the geometry and flow rate, using a forward and inverse modeling in the wavelet domain [48]. The hydraulic conductivity and the thickness of the aquifer can also be estimated using an inversion scheme for surface SP generated by flow pumping, taking into account the conducting steel casing [49]. Electric potential variations have also been associated with lake level variations, showing a magnitude of 2 mV per meter of water level change between a one km wide ridge separating two lakes [50]. The detection of changes in the flow rate of expelled fluids in accretionary prisms by monitoring of electric and magnetic fields has been discussed. The modeling of electrokinetics at the Nankai trough showed that fluid flow rate variations of 20% could be detected by a variation of 3 mV and about 2 nT at 600 m depth in a borehole [51]. Moreover, recent modeling has shown that SP could detect at distance the propagation of a water-front in a reservoir [52].

The interpretation of all these observations has been possible through developments of the theory, direct modellings, and inverse problems. The interpretation of SP observations needs to resolve the poisson equation for the electric streaming potential, considering a total electric potential [53–56]. Direct modelling has been developed [51, 57, 58]. Moreover, SP observations have been interpreted in the wavelet domain in order to identify location and intensity of the source of the underground hydraulic flows [14, 15, 59, 60]. Gibert & Sailhac [61] have commented on Patella's correlation approach to demonstrate that the so-called probability of tomography defines images of SP data in the wavelet domain that must not be interpreted as underground images of SP sources. They pointed out that an appropriate inversion is necessary to achieve underground images. Numerous recent studies showed that these inverse problems still need further developments [62–65].

Because of similarity between the electrical potential with the pressure behavior, it has been proposed also to use SP measurements as an electrical flow-meter [66]. Moreover, the electrokinetic properties have been used to predict the permeability. Li et al. [67] defined an electrokinetic permeability which can be deduced from the rock conductivity, the electroosmosis coefficient, and the streaming potential coefficient. Recently, Glover et al. [68] proposed a new prediction for the permeability by comparing an electrical model derived from the effective medium theory to an electrical model for granular medium. And, it has also been proposed to deduce the permeability of the Nojima fault (Japan) using the self-potential observations in surface when water is injected into a well of 1800 m depth [69].

The origin of seismoelectromagnetic conversions is also the electrokinetic effect, which is in this case induced by a seismic wave propagation. Two kinds of mechanical to electromagnetic conversions exist: (1) The electrokinetic signal which travels with the acoustic wave; (2) The interfacial conversion occurring at contrasts of physical properties such as permeability.

The second kind of conversion can be used to detect contrasts in physical properties in the crust. A seismic source placed at the surface can induce a seismic wave propagation downward up to the interface (Figure 1). There is a charge

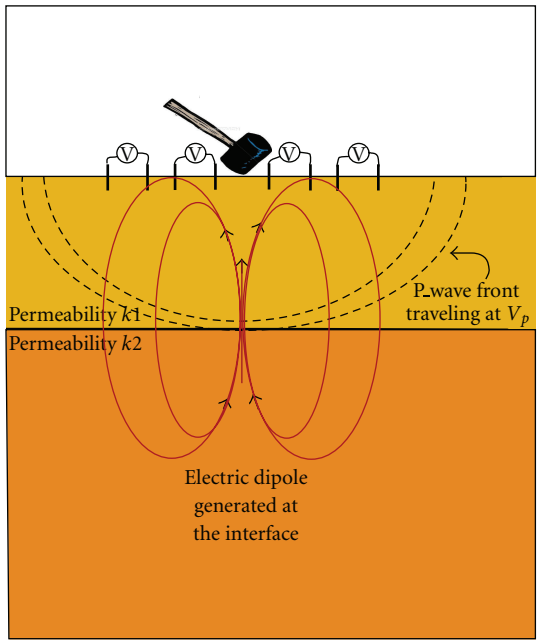

Figure 1: The seismic waves (induced by a hammer strike) propagate up to the interface where an electric dipole is generated because of the contrast in permeability (or in other physical properties). This electromagnetic wave can be detected at the surface by measuring the difference of the electrical potential V between electrodes. Picking the time arrival allows to know the depth of the interface.

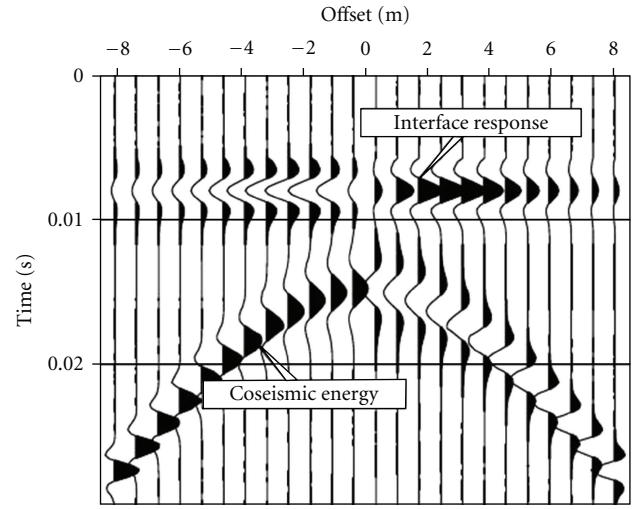

Figure 2: Model of the seismoelectric response to a hammer strike on the surface at position zero (from Haines [77]). The seismoelectric signal is shown as measured at the surface along a line centered on the seismic source. The interfacial signal is related to a contrast between properties of the media, such as the permeability.

inbalance that causes a charge separation on both sides of the interface because of the difference in the physical properties. This acts as en electric dipole which emits an electromagnetic wave that travels with the speed of the light in the medium and that can be detected at the surface (Figure 2). The velocity of the seismic wave propagation is deduced by surface measurements of the soil velocity. Then the depth of the interface can be deduced by picking the time arrival of the electromagnetic wave. The amplitude of the seismoelectric signals is usually low from 100 μV to mV. Then signal processing needs filtering techniques such as Butler & Russell [70, 71]. The advantage of this method is to detect the contrasts in physical properties at depth from few meters to few hundreds of meters [72–76].

The aim of this paper is to give the background needed to understand this special issue on "Electrokinetics in Earth Sciences". We detail the theoretical background for the electrical double-layer and for the transport equations used to study the streaming potential and the seismoelectromagnetic conversions. We specially point out the use of self-potential for geothermal applications.

2. Electrokinetics: Theoretical Background

2.1. Electrical Double Layer. Fluid flow in porous media can lead to electrokinetic effects. Indeed the presence of ions within the fluid can induce electric currents when water flows. This effect is directly related to the existence of an electrical double layer between the rock and the fluid. Minerals forming the rock develop an electric double-layer when in contact with an electrolyte, usually resulting from a negatively charged mineral surface. An electric field is created perpendicular to the surface of the mineral which attracts counterions (usually cations) and repulses anions in the vicinity of the pore matrix interface. The electric double layer (Figure 3) is made up of the Stern layer, where cations are adsorbed on the surface and the Gouy diffuse layer, where the number of counterions exceeds the number of anions [78–80].

The fluid contains M_i ionic species with valence z_i ($i = 1, \ldots M_i$) and number density N_i^b (the number of species-i ions per unit volume) in the bulk solution far from any charged surface. The distribution of the electrical potential ϕ within the electrical double layer perpendicular to the solid surface can be calculated resolving the following Poisson's equation:

$$\nabla^2\phi = -\frac{\rho}{\epsilon_f}, \tag{1}$$

where ϵ_f is the dielectric constant of the fluid, and the charge density ρ can be expressed using a Boltzmann distribution for the ionic species within the fluid

$$\rho = \sum_{i=1}^{M} e z_i N_i^b \exp\left(-\frac{e z_i \phi}{kT}\right), \tag{2}$$

where k is the Boltzmann constant, $-e$ is the charge of an electron, and T is the temperature. It is often assumed that the Poisson-Boltzmann equation governing the equilibrium charge clouds can be linearized. Assuming $e\phi/kT \ll 1$, the Poisson's equation becomes

$$\nabla^2\phi = \kappa^2\phi, \tag{3}$$

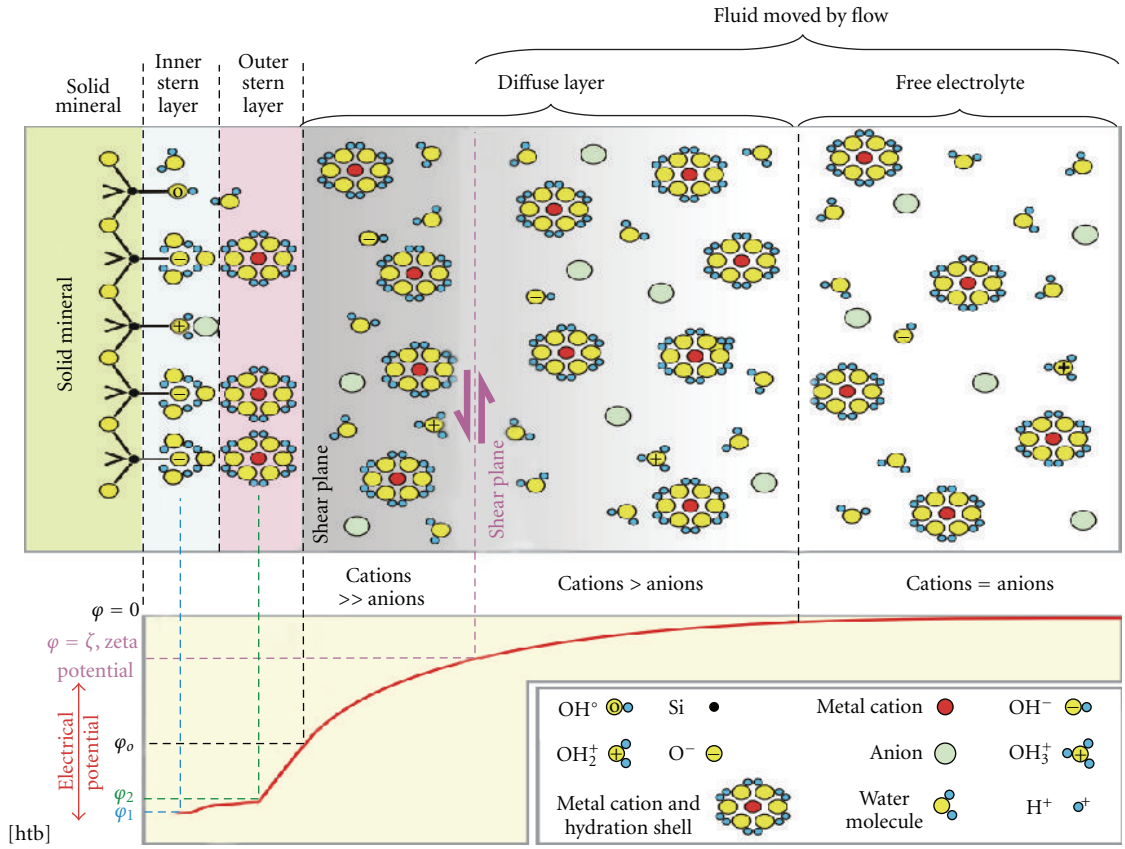

FIGURE 3: Electric double layer, first published in [81]. The solid mineral presented is the case of silica. At pH above the isoelectric point, the cations are adsorbed within the Stern layer; there is an excess of cations in the diffuse layer. The zeta potential is defined at the shear plane. The fluid flow creates a streaming current which is balanced by the conduction current, leading to the streaming potential.

with κ^{-1} is the Debye length, which is a measure of the thickness of the double diffuse layer, typically of the order of a few nm

$$\frac{1}{\kappa^{-2}} = \sum_{i=1}^{M} \frac{e^2 z_i^2 N_i^b}{\epsilon_f kT}. \tag{4}$$

The electrical potential ϕ at a distance x from a charged surface is therefore

$$\phi(x) = \zeta \exp(-\kappa x), \tag{5}$$

and ζ is called the zeta potential and is the electrical potential at the shear plane (for further details see Pride [82]).

The charge density at the surface of the minerals results from surface complexation reactions. The quartz surface can be modelled with silanol $>SiOH$ group [79]. The potential-determining ions OH^- and H^+ are adsorbed onto the surface of the mineral and determine the charge density on the inner plane (see Figure 3). The surface charge is therefore dependent on the pH. There exists a pH for which the total surface charge is zero; this is the point of zero charge and pH is called pH_{pzc} [83, 84]. The charge is positive for $pH < pH_{pzc}$ and negative for $pH > pH_{pzc}$. In this case, this electrokinetic effect is zero. The pH_{pzc} for quartz is in the range $2 < pH_{pzc} < 4$ [85, 86]. The calcite surface can be modelled with $>CaOH$ and $>CO_3H$ groups. Carbonate ions and Ca^{2+} are the determining potential ions. The electrokinetic behavior on carbonates is more complicated. The pH_{pzc} varies from 7 to 10.8 according to the authors [87]. It is possible to model simple interfaces and to calculate zeta potential in simple cases [88]. This modeling can be performed assuming the triple-layer model (TLM) which distinguishes three planes to describe the electric double layer: the inner Helmholtz plane for counter ions directly bound to the mineral (assumed to be chemically adsorbed), the outer Helmholtz plane for weakly bound counter ions (assumed to be physically adsorbed), and a d-plane associated with the smallest distance between the mineral surface and the counter ions in the diffuse layer. It has been proposed that the slipping plane lies near the distance of closest approach of dissociated ions, and that the ζ potential can be calculated as the potential on this plane [83].

The streaming current is due to the motion of the diffuse layer induced by a fluid pressure difference along the interface. This streaming current is then balanced by the conduction current, leading to the streaming potential.

2.2. Theoretical Background for Streaming Potentials. The different flows (fluid flow, electrical flow, heat flow, concentration flow) are governed by the general equation

$$\mathbf{J}_i = \sum_{j=1}^{N} \mathcal{L}_{ij} \mathbf{X}_j, \tag{6}$$

which links the forces $\mathbf{X}_j$ to the macroscopic fluxes $\mathbf{J}_i$, through transport coupling coefficients $\mathcal{L}_{ij}$ [89].

Considering the coupling between the hydraulic flow and the electric flow, assuming a constant temperature and no concentration gradients, the electric current density $\mathbf{J_e}$ [A · m^{-2}] and the flow of fluid $\mathbf{J_f}$ [m · s^{-1}] can be written as the following coupled equation:

$$\mathbf{J_e} = -\sigma_0 \nabla V - \mathcal{L}_{ek} \nabla P. \tag{7}$$

$$\mathbf{J_f} = -\mathcal{L}_{ek} \nabla V - \frac{k_0}{\eta_f} \nabla P, \tag{8}$$

where P is the pressure that drives the flow [Pa], V is the electrical potential [V], σ_0 is the bulk electrical conductivity [S · m^{-1}], k_0 the bulk permeability [m^2], η_f the dynamic viscosity of the fluid [Pa · s], and $\mathcal{L}_{ek}$ the electrokinetic coupling [A Pa^{-1} m^{-1}]. Therefore, the first term in (7) is the Ohm's law, and the second term in (8) is the Darcy's law. The coupling coefficient is the same in (7) and (8) because the coupling coefficients must satisfy the Onsager's reciprocal relation in the steady state. This reciprocity has been verified on porous materials [90, 91] and on natural materials [92].

Without direct electric current source, the conservation of the total current density implies

$$\nabla \cdot \mathbf{J}_e = 0, \tag{9}$$

which is the Poisson's equation for the electrical potential V. If the medium is heterogeneous, (9) has to be computed taking into account the sources located at boundaries formed by electrical conductivities and streaming coefficients contrasts [93]. In the case of an homogeneous medium (9) leads to the simplified Poisson's equation

$$\nabla^2 V = C \nabla^2 P. \tag{10}$$

The streaming potential coefficient C_{s0} [V · Pa^{-1}] is defined when the electric current density $\mathbf{J_e}$ is zero, leading to

$$\frac{\Delta V}{\Delta P} = -\frac{\mathcal{L}_{ek}}{\sigma_0} = C_{s0}. \tag{11}$$

This coefficient can be measured by applying a driving pore pressure ΔP to a porous medium and by detecting the induced electric potential difference ΔV. The driving pore pressure induces a streaming current (second term in (7)) which is balanced by the conduction current (first term in (7)) which leads to the electric potential difference ΔV that can be measured. In the case of a unidirectional flow through a cylindrical saturated porous rock, this coefficient can be expressed as [32, 94]

$$C_{s0} = \frac{\epsilon_f \zeta}{\eta_f \sigma_{\text{eff}}}. \tag{12}$$

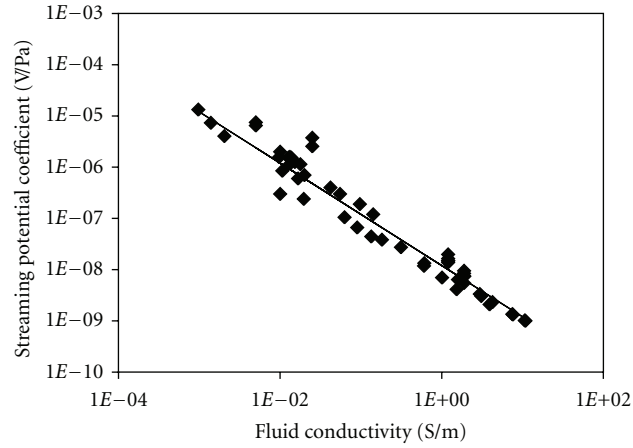

Figure 4: Streaming potential coefficient from data collected (in absolute value) on sands and sandstones at pH 7-8 (when available) from Ahmad [100]; Li et al. [67]; Jouniaux and Pozzi [101]; Lorne et al. [86]; Pengra et al. [102]; Guichet et al. [21]; Perrier and Froidefond [103]; Guichet et al. [88]; Ishido and Mizutani [96]; Jaafar et al. [98]. The regression (black line) leads to $C_{s0} = -1.2 \times 10^{-8} \sigma_f^{-1}$. A zeta potential of −17 mV can be inferred from these collected data from Allègre [24].

with the fluid electrical permittivity ϵ_f [F·m^{-1}], the effective electrical conductivity σ_{eff} [S·m^{-1}] defined as $\sigma_{\text{eff}} = F\sigma_0$ with F the formation factor and σ_0 the rock conductivity which can include a surface conductivity. The potential ζ[V] is the zeta potential described as the electrical potential inside the EDL at the slipping plane or shear plane (i.e., the potential within the double-layer at the zero-velocity surface).

The streaming coefficient is described by the well-known Helmholtz-Smoluchowski equation [95] when the surface conductivity can be neglected compared to the fluid conductivity ($F\sigma_0 = \sigma_f$)

$$C_{s0} = \frac{\epsilon_f \zeta}{\eta_f \sigma_f}. \tag{13}$$

The assumptions are a laminar fluid flow, identical hydraulic, and electric tortuosity. The influencing parameters on this streaming potential coefficient are therefore the dielectric constant of the fluid, the viscosity of the fluid, the fluid conductivity and the zeta potential itself depending on rock, fluid composition, and pH [86, 88, 94, 96–99]. At a given pH, the most influencing parameter is the fluid conductivity. Numerous measurements of the streaming potential on sand have been published, that can lead to the relation $C_{s0} = -1.2 \times 10^{-8} \sigma_f^{-1}$ (Figure 4). A zeta potential of −17 mV can be inferred from these collected data, assuming all the other parameters constant.

2.3. Theoretical Background for Seismoelectromagnetics. The origin of the seismoelectromagnetic conversion is also the electrokinetic effect, which is in this case induced by seismic wave propagation. The relative motion between the fluid and the rock matrix is induced by the seismic wave propagation. The reciprocal process also occurs; the electromagnetic waves

couple to displacement fields and they generate seismic waves at electrical/mechanical interfaces [104, 105]. In this case, the electrokinetic coefficient depends on the frequency ω as the dynamic permeability $k(\omega)$ [106]. Pride [82] developed the theory for the coupled electromagnetics and acoustics of porous media, coupling the electric field in Maxwell's relations to the displacement fields in Biot's equations. The transport relations ([82, equations (250) and (251)]) are

$$\begin{aligned} \mathbf{J_e} &= \sigma(\omega)\mathbf{E} + \mathcal{L}_{ek}(\omega)\left(-\nabla p + \omega^2\rho_f \mathbf{u_s}\right), \\ -i\omega\mathbf{J_f} &= \mathcal{L}_{ek}(\omega)\mathbf{E} + \frac{k(\omega)}{\eta}\left(-\nabla p + \omega^2\rho_f \mathbf{u_s}\right). \end{aligned} \tag{14}$$

The electrical fields and mechanical forces which induce the electric current density $\mathbf{J_e}$ and the fluid flow $\mathbf{J_f}$ are, respectively, $\mathbf{E}$ and $(-\nabla p + i\omega^2\rho_f \mathbf{u_s})$, where p is the pore-fluid pressure, $\mathbf{u_s}$ is the solid displacement, $\mathbf{E}$ is the electric field, ρ_f is the pore-fluid density, and ω is the angular frequency. The electrokinetic coupling $\mathcal{L}_{ek}(\omega)$ is now complex and frequency-dependent and describes the coupling between the seismic and electromagnetic fields [82, 107]

$$\begin{aligned} \mathcal{L}_{ek}(\omega) = \mathcal{L}_{ek}\Bigg[& 1 - i\frac{\omega}{\omega_c}\frac{m}{4}\left(1 - 2\frac{d}{\Lambda}\right)^2 \\ & \times\left(1 - i^{3/2} d\sqrt{\frac{\omega\rho_f}{\eta}}\right)^2\Bigg]^{-1/2}, \end{aligned} \tag{15}$$

where m and Λ are geometrical parameters of the pores (Λ is defined in Johnson et al. [108] and m is in the range 4–8), d is the Debye length. The transition frequency ω_c defined in the Biot's theory separates the viscous and inertial flow domains and depends on the permeability k_0. The frequency-dependence of the streaming potential coefficient has been studied [107, 109–115] mainly on synthetic samples and recently on sand [116]. Both models [117–123] and laboratory experiments [116, 124–129] have been developed on these seismoelectromagnetic conversions. Over the past decades, seismoelectromagnetic phenomena have been observed in the field [130–132], and increasing successful field experiments have been reported in recent years [73, 75, 119, 133–136].

3. Geothermal Applications

3.1. Self-Potential Associated with Natural Hydrothermal Circulation. The SP method has attracted increasing interest in geothermal prospecting. Among the various mechanisms which can cause SP in geothermal areas, the most important appear to be streaming potentials [96, 137–139]. Electrokinetic effects are almost certainly responsible for the production-induced changes in SP which take place after a field is developed [57]. Repetitive SP surveying of geothermal fields during exploitation represents a promising tool for geothermal field monitoring and resource management.

During the past two decades, numerical modeling of SP generation has been undertaken in geothermal and hydrological studies [55, 57, 58, 140]. The method proposed by Ishido and Pritchett [57] applies the so-called "*EKP-postprocessor*" to the results of an unsteady thermohydraulic reservoir simulation. First, it calculates the distributions of pertinent parameters such as the electrokinetic coupling $\mathcal{L}_{ek}$, the electrical conductivity, and the drag current density using the results from the reservoir simulation. Next, the postprocessor calculates the electric potential distribution by solving the Poisson's equation within a finite-difference grid with appropriate boundary conditions.

Figure 5 shows the SP distribution expected to arise from natural hydrothermal convection. A positive SP anomaly is present above the central upflow region. This is produced by positive-charge accumulation due to the large reduction in the streaming potential coefficient along the upflow path. Contrasting large negative anomalies appear in the peripheral regions where meteoric water flows downward. This is produced by the descending meteoric water which removes positive charge from the neighborhood of the ground surface. The peripheral negative anomalies are larger in magnitude than the central positive anomaly due to relatively low electrical conductivity. A representative flow rate (Darcy velocity) is 10^{-8} m/s in this case. In cases with higher flow rate, the magnitudes of both the positive and negative anomalies will be increased. However, the magnitude of central positive anomaly will not become significantly larger than 100 mV since the driving force for the upflow is usually less than several percent of the hydrostatic pressure gradient [141], and the electrical conductivity of upflowing fluid is relatively high due to dissolved species.

Figure 6 shows the measured SP profile across the Nigorikawa caldera [142]. SP is high within the caldera where upflows take place, but the surrounding area is characterized by more distinct negative SP anomalies. These features are well reproduced by the above calculation (Figure 5(d) using "*EKP-postprocessor*" Ishido & Pritchett [57]). Similar SP features were observed at the mud volcano area in Yellowstone [137], the Kirishima field in Japan [143], the Mokai and Rotokawa fields in New Zealand [144], and so forth.

The results of the calculation shown in Figure 5 confirmed the results of "semiquantitative" modeling by Ishido [142] (an outline of which is given in Ishido et al. [145]; Zlotnicki & Nishida [146]). In the case of source-free fluid flow driven by buoyancy, the primary conduction current source (which causes the SP at the earths surface) appears at the boundary between regions of different electrokinetic coupling ($\mathcal{L}_{ek}$). The magnitude of the conduction current source is given by the difference in the coupling coefficient across the boundary multiplied by the pressure gradient perpendicular to the boundary. Ishido [142] assumed that the coupling coefficient depends both on temperature and on pore-water chemistry based upon the experimental results of Ishido & Mizutani [96].

Better understanding of the zeta potential and/or streaming potential coefficient is fundamentally important in quantitative modeling of electrokinetic potentials associated with subsurface fluid flow. Recent laboratory measurements under high-temperature conditions [147–149], high-salinity conditions [98], and liquid/gas two-phase conditions [21, 22] are particularly relevant to modeling studies for geothermal and

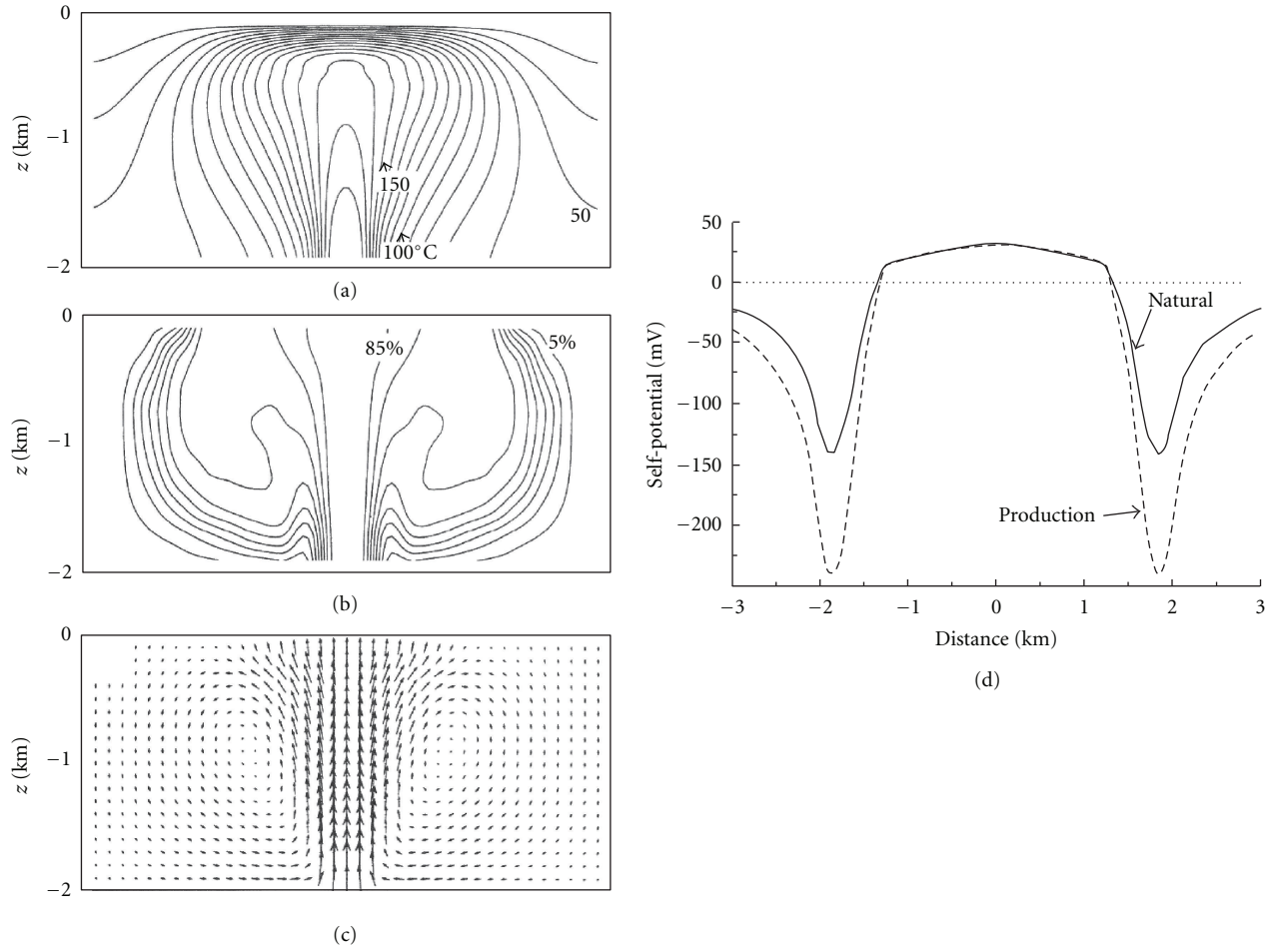

Figure 5: Results of reservoir simulation: natural-state distributions of (a) temperature (contour interval 10°C), (b) mass fraction of "source fluid", and (c) fluid mass flux. Earth-surface SP distributions computed by the so-called "*EKP postprocessor*" for this natural state (solid curve), and for a subsequent exploited state (broken curve), are shown in (d), after [57].

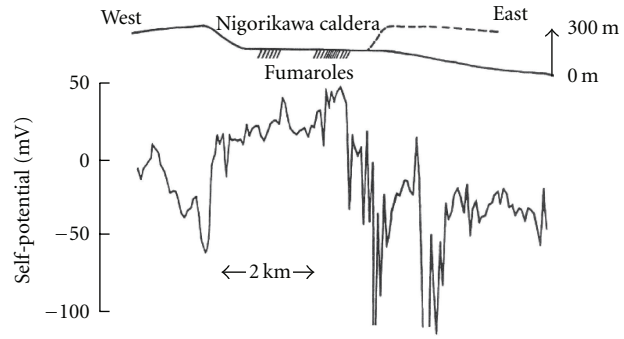

Figure 6: Topographic section and self-potential profile across the Nigorikawa caldera measured in 1978, after [142].

volcanic areas. In addition to measuring the coupling coefficients of representative rock samples from survey areas (e.g., Jouniaux et al. [94]; Hase et al. [150]; Aizawa et al. [151]; Onizawa et al. [18]), basic phenomenological measurements such as the determination of the dependency of the streaming potential coefficient upon pore size [152] are essential.

3.2. "W"-Shaped SP Profiles across Volcanoes. Numerous SP surveys of active volcanoes have been carried out during the past thirty years. Obvious positive-polarity SP anomalies have often been observed around volcanic craters or vents; for example, Kilauea [153], Akita Yake-yama [145], Unzen [154], Miyake-jima [155, 156], Izu-Oshima [16], La Fournaise [157], Mt. Fuji [158], Misti [12], and Mt. Aso [13]. In addition to these, various other types of SP anomalies were reported on active volcanoes [11, 146, 159, 160]. In cases like Miyake-jima, Izu-Oshima, Mt. Fuji, Mt. Aso, Misti and La Fournaise [9], SP first decreases several hundred millivolts, sometimes more than one volt, as one climbs the slopes of the volcano, then rapidly recovers to the level measured on the flank of volcano as the summit crater is approached. Consequently, the entire SP profile along a survey line starting from the foot, passing near the summit, and reaching the foot on the opposite side often has the shape of the letter "W".

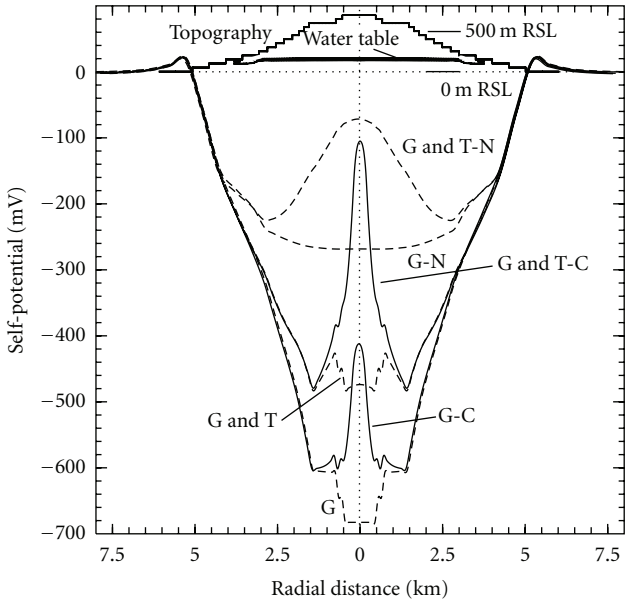

Figure 7: Self-potential distributions computed from numerical simulation results of thermohydraulic processes within a volcanic body, after [17]. Cases "G-" and "G and T-" correspond to the conditions of "steady-state of topography-driven groundwater flow" and "100 years after continuous heating of central conduit below sea level", respectively. For cases "-C", a shallow conductor above the water table is assumed. For cases "-N", the drag current in the unsaturated zone is neglected. The "W"-shaped SP profile observed at Izu-Oshima volcano is reproduced by case "G and T-C". The sketch in the upper part of the figure illustrates the earth surface topography and the water table elevation.

Numerical simulations by Ishido [17], which were based on a conceptual model of Izu-Oshima volcano, show that the primary cause of the "W"-shaped SP distribution is a combination of the electrokinetic drag current associated with the downward liquid flow in the unsaturated and underlying saturated layers and the presence of a shallow conductor near the volcano summit. If the shallow conductor contacts a deep conductive layer, this conductive structure provides a current path between the low-potential shallow and high-potential deep regions, resulting in substantial increase in SP around the summit (Figure 7). The calculated W-shaped profile is stable even with periodic groundwater recharge, which is consistent with field observations.

Assuming a plausible value of zeta potential and liquid-saturation dependency of drag current, the terrain-related SP is calculated as about −1 mV/m, which is typical of the magnitudes observed at a number of volcanoes. Two ways have been proposed to interpret SP generation due to gravity-driven water flow; the first considers only downward percolation of vadose-zone water to the water table [8], and the second considers situations where the effects of water flow in the deeper saturated zone predominate [161, 162]. In the simulation results shown in Figure 7, gravity-driven water flows in both the unsaturated and underlying saturated zones contribute to generate the terrain-related SP. Concerning SP generation in the unsaturated zone, a vertical potential gradient of −1 to −2 mV/m was observed by multiple Ag/AgCl electrodes installed in a 100 m research hole drilled in the eastern part of the caldera floor at Izu-Oshima (N. Matsushima, personal communication). A similar vertical SP gradient averaging −1.35 mV/m was observed for the upper 488 m interval above the water table in a research hole at Kilauea's summit [163]. This potential gradient is thought to be produced by a substantial downward flow of meteoric water in the unsaturated zone, which is suggested by uniform temperatures near 25°C in the subsurface region above the water table [163].

The effect of drag current associated with hydrothermal upflow is shown minor compared to the effect of the heterogeneous conductivity structure, especially if the fluid circulates to great depth and is highly saline. Upflows of vapor or volcanic gas to the summit crater can reduce the drag current associated with meteoric water downflow within the volcanic conduit [16] and will also provide a secondary contribution to the increased SP near the summit (Figure 7). Onizawa et al. [18] carried out 3-D numerical simulations of groundwater flow due to meteoric water infiltration and the resulting induced SP to understand the fundamental grounwater flow regime and the causes of the SP observed at Izu-Oshima. They reproduced the overall pattern of the observed SP distribution by incorporating a heterogeneous resistivity structure derived from Audio Magneto Telluric (AMT) measurements.

Aizawa et al. [164] found that 2-D resistivity sections obtained by AMT surveys in five large Japanese stratovolcanoes (Iwate, Iwaki, Nasu, Nantai, and Nikko-Shirane) correlate closely with SP measurements [160]. Extensive conductors extend downward from shallow levels on slopes that lack SP anomalies, whereas the top of the conductor is relatively deep on slopes where large SP minima are observed. They confirmed the plausibility of the proposed conceptual model based on numerical simulations of a hydrothermal system with sealing layers and meteoric water recharge and reproduced the observed relationship between the SP and resistivity data.

The calculated high SP amplitude near the summit is sensitive to the conductivity structure, which is thought to change over time due to volcanic activities such as magma ascent, degassing, and development of hydrothermal convection [165, 166]. This is thought to be at least partly responsible for the temporal SP variations observed at Kilauea [153], Unzen [154] and other volcanoes.

3.3. SP Changes Induced by Geothermal Fluid Production and Reinjection. When a sink or source of fluid is present within a reservoir as a result of production or reinjection of geothermal fluids, a surface electric potential anomaly can be produced through electrokinetic coupling if the following conditions are satisfied. First, there must be a boundary separating regions of differing streaming potential coefficient C_{s0} (denoted as C hereafter); second, there must be a nonzero component of pressure gradient parallel to this boundary [53, 167]. A temperature boundary, a boundary between regions of different pore water chemistry, and/or a contact of different rock formations are the most likely causes for discontinuities in the value of C in a geothermal reservoir

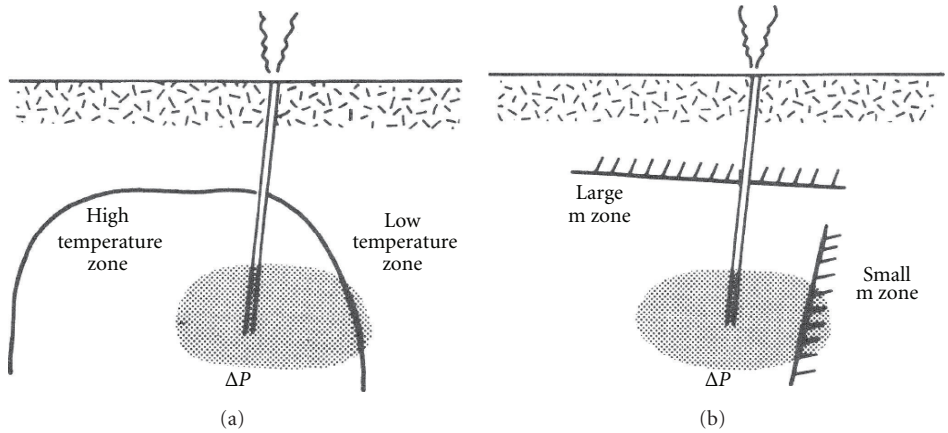

Figure 8: Models for production-induced SP change, after [145]. (a) High-low temperature interface, or (b) large-small pore hydraulic radius (m) interface acts as a boundary between regions of differing streaming potential coefficient. Shaded region: zone of production-induced pressure disturbance.

(Figure 8). When a propagating pressure disturbance induced by production and/or injection of fluids reaches a boundary between regions of differing C in the reservoir, an SP change will appear at the earth's surface [145].

A quantitative and physically reasonable method for calculating SP anomalies near C boundaries was described by Fitterman [53] based on earlier work by Nourbehecht [167]. A total electric potential is defined by

$$\psi = V - CP, \tag{16}$$

such that the current flow is given by

$$\mathbf{J_e} = -\sigma_0 \nabla \psi. \tag{17}$$

In the absence of current sources, $\nabla \cdot \mathbf{J}_e = 0$ and for homogeneous regions,

$$\nabla^2 \psi = 0, \tag{18}$$

with boundary conditions of continuity of normal current flow

$$\sigma_0 \mathbf{n} \nabla \psi|_1^2 = 0 \tag{19}$$

and discontinuity of total electric potential at interfaces equal to the difference in C times the pressure

$$\psi|_1^2 = -C|_1^2 P = S, \tag{20}$$

where S is a generalized source function ($X|_1^2$ means the jump in X across the boundaries). The discontinuity of ψ is the result of V and P being continuous while C is discontinuous. The ψ distribution can be calculated as the potential produced by a surface distribution of current dipoles with surface dipole density $\sigma_0 S$ along the interface [168]. If the boundary is nearly vertical, the SP anomaly will be dipolar in waveform. When P is negative (positive), this dipole source points towards the side of larger (smaller) C. If the boundary condition at the earths surface is P = constant or the pressure change is confined at depth, the SP anomaly is brought about solely by this dipole source; therefore no SP anomaly will appear at the earths surface if the C distribution is homogeneous. This is also true for gravity-driven groundwater flow if the fluid density is constant in the entire region. For example, SP depends only on ground surface elevation for a fully saturated region of homogeneous C [169]; this is true even if the permeability distribution is heterogeneous and thus pressure gradient normal to a permeability boundary is discontinuous.

The Mori geothermal power plant was built in the Nigorikawa caldera in 1982 and has been in continuous operation since. Comparing the results of SP surveys in 1978, 1981, and 1984, Ishido et al. [145] found a production-induced SP change (Figure 9). The dipolar change in SP appears over the principal zone of fluid production. This observed change is believed to be generated by underground fluid flows resulting from the production (and reinjection) of geothermal fluids through electrokinetic coupling and partly reproduced in the modeling results shown Figure 5. The upflowing hot water in the central region is relatively saline, so the magnitude of the local streaming potential coefficient $|C_{\text{res}}|$ is thought to be smaller than for the fresh water in the peripheral region $|C_{\text{per}}|$ (so that $C_{\text{per}} < C_{\text{res}} < 0$). So, the dipole source for ψ appearing along the nearly vertical C boundary is thought to point into the central region, resulting in increase and decrease in SP in the central and peripheral areas, respectively.

This is one of the possible interpretations. Another candidate for a boundary between regions of differing C is thought to be the interface between the reservoir and overlying caprock. Yasukawa et al. [170] carried out modeling studies to interpret the observed SP changes associated with a short-term field-wide shut-in of production and reinjection wells at the Mori power plant. In their model, the streaming potential coefficient is assumed as $C_{\text{res}} < C_{\text{cap}} < 0$ (here, C_{res} and C_{cap} are the streaming potential coefficient of reservoir and caprock regions, resp.). So the observed central increase and peripheral decrease in SP, which are also reproduced

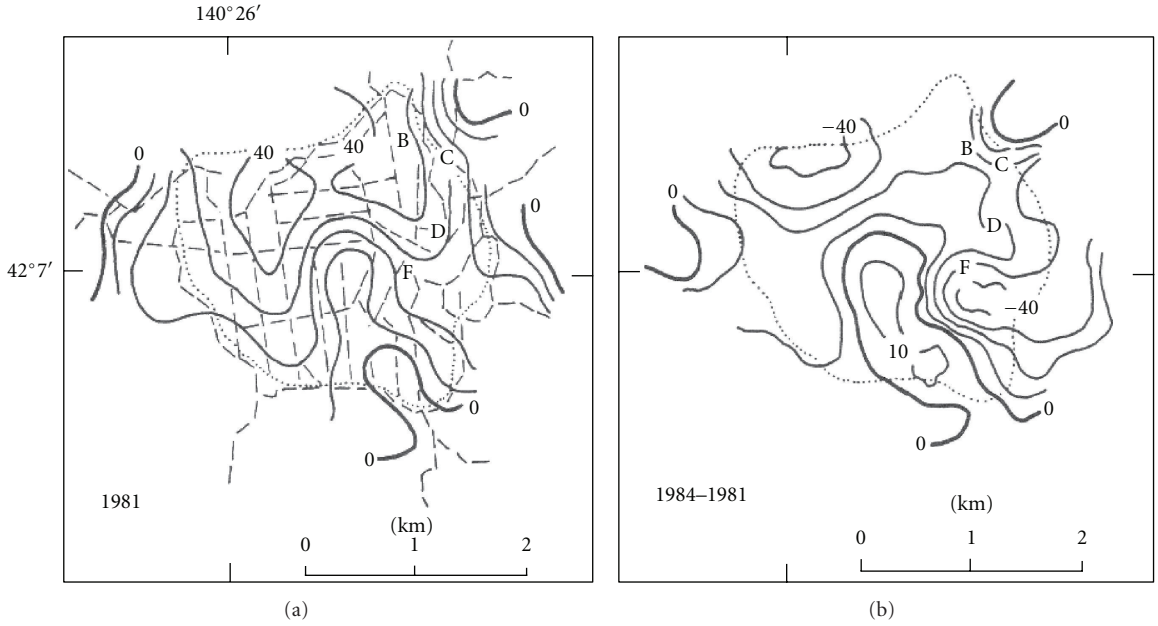

Figure 9: Self-potential distributions in the Nigorikawa caldera (a) measured in 1981 and (b) difference in SP distribution between 1981 and 1984, after [145]. Contour interval is 10 mV. Broken lines shown in (a) denote survey lines used for 1981 and 1984 surveys (the data sampling intervals are 100 m). The edge of the caldera floor is indicated by the dotted lines. B, C, D, and F represent well sites.

in the numerical modeling, are interpreted as induced by pressure decrease (due to production) and increase (due to reinjection), respectively, along the interface.

In many geothermal reservoirs, substantial production-induced expansion of the vapor-dominated zone (due to reservoir pressure decline) takes place during the early stages of field operation. Just below the vapor zone, vigorous boiling occurs and counterflows of vapor (upward) and liquid (downward) are produced. This downward flow of the liquid phase carries drag current with it and brings about a negative SP change on the ground surface [57]. Preliminary modeling studies [171, 172] show that the observed SP changes at the Okuaizu field in Japan (Figure 10) can be explained by this process. An interpretation based on the total electric potential is also available for this process [57]. At Okuaizu, fractured reservoirs develop along nearly vertical faults within country rocks of very low permeability. The magnitude of the streaming potential coefficient of the country rocks (C_{ctr}) is thought to be substantially smaller than that of the reservoir rocks (C_{res}) [32, 97]. So the $C_{res} < C_{ctr} < 0$ inequality will not change, irrespective of C_{res} change caused by increasing vapor saturation, so long as the liquid phase remains mobile. Then, pressure decline due to a vertically-extensive boiling zone brings about a negative SP change at the earth's surface.

Since the possibility always exists that production-induced SP changes overlap the natural SP distribution associated with the undisturbed state, care must be exercised in interpreting SP data from areas where fluid production is taking place. Furthermore, sources of noise associated with newly drilled wells, deployed pipelines, and so forth need to be evaluated. At the Sumikawa field in Japan, SP surveys were carried out twice before the startup of the geothermal power

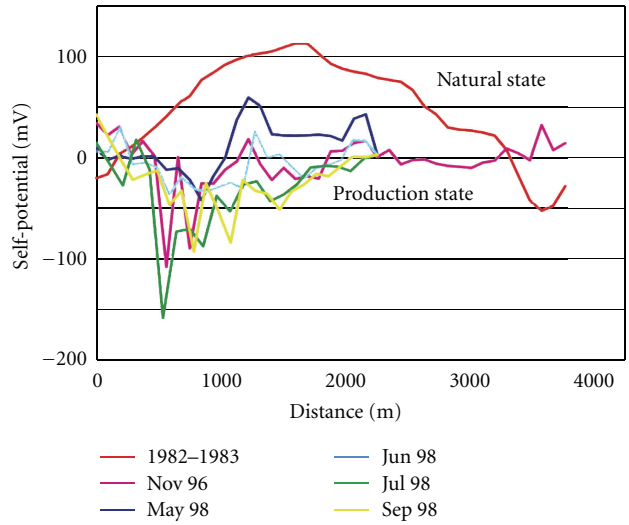

Figure 10: SP profile along a survey line passing through the central part of the Okuaizu geothermal field in Japan. The red line shows the SP profile under natural state conditions, measured in 1982-83. The survey in November 1996 was carried out about 1.5 years after start-up of the Yanaizu-Nishiyama power station. The repeated surveys in 1998 were carried out after 2 months shut-in of production wells in April and May 1998, after [171, 172].

station in 1995 and again three times afterwards [173]. Unfortunately, no data free from "artificial" noise are available except that from the first survey in 1983. Negative potentials of up to several hundred millivolts are present near metallic artifacts such as well casings and pipelines.

The pipelines, which were deployed after 1983 along the principal survey lines used in the 1983 survey, are connected to the wellheads and are in electrical contact with the ground surface at various locations. Continuous SP measurements near the wellheads and pipelines show that temporal potential changes correspond to temporal temperature variations near the surfaces of the metallic structures, which could be explained by a simple "redox" model [174]. Other important noise sources to be taken into account for field measurements are discussed by Corwin and Hoover [139].

To estimate magnetic fields associated with fluid flows in geothermal reservoirs, "*EKP postprocessor*" calculations were carried out applying the Biot-Savart law to the distributions of drag and conduction current densities [175]. Their results suggest that magnetic anomaly magnitudes caused solely by electrokinetic coupling are too weak to be observed, either for natural or exploited conditions. However, this does not rule out the appearance of observable magnetic fields due to electrokinetic coupling in other situations where significant fluid flow takes place in a region with heterogeneous and/or anisotropic rock properties (e.g., Mizutani & Ishido [176]; Zlotnicki & Mouel [177]).

In addition to electrokinetic (EK) coupling, several other effects such as thermoelectric coupling and chemical diffusion potential cannot be ruled out as possible causes of self-potential anomalies in geothermal fields. However, EK phenomena are almost certainly responsible for the production-induced changes in SP that take place after a field is developed. No other effects will play significant roles, since production-induced changes in the distributions of fluid chemistry and temperature will be minor compared to flow pattern changes, especially in the early stages of exploitation. SP monitoring such as that carried out at Okuaizu [171, 178] is thought to be useful for history matching studies, particularly to improve mathematical models of fractured reservoirs [172, 179, 180].

4. Conclusion

A lot of observations have been performed these last decades, both Self-Potential and seismoelectromagnetics observations. We detailed the theoretical background needed to interpret these observations and pointed out the use of self-potentials for geothermal applications. We tried to provide an extensive overview and to mention the related key publications. We hope that this tutorial is useful to better understand the papers published in the special issue "Electrokinetics in Earth Sciences" of International Journal of Geophysics. Further improvement should come from studies on signal processing, on inverse problems, and from technical development.

Acknowledgments

This paper was supported by the French National Scientific Center (CNRS) and by REALISE the "Alsace Region Research Network in Environmental Sciences in Engineering" and the Alsace Region. The paper on geothermal applications was supported by the Geological Survey of Japan and the Institute for Geo-Resources and Environment, the National Institute of Advanced Industrial Science and Technology.

References

[1] J. T. G. Overbeek, "Electrochemistry of the double layer," in *Colloid Science, Irreversible Systems*, H. R. Kruyt, Ed., vol. 1, pp. 115–193, Elsevier, 1952.

[2] L. Jouniaux, A. Maineult, V. Naudet, M. Pessel, and P. Sailhac, "Review of self-potential methods in hydrogeophysics," *Comptes Rendus Geoscience*, vol. 341, no. 10-11, pp. 928–936, 2009.

[3] G. Petiau and A. Dupis, "Noise, temperature coefficient, and long time stability of electrodes for telluric observations," *Geophysical Prospecting*, vol. 28, no. 5, pp. 792–804, 1980.

[4] G. Petiau, "Second generation of Lead-lead chloride electrodes for geophysical applications," *Pure and Applied Geophysics*, vol. 157, no. 3, pp. 357–382, 2000.

[5] F. Moreau, D. Gibert, and G. Saracco, "Filtering nonstationary geophysical data with orthogonal wavelets," *Geophysical Research Letters*, vol. 23, no. 4, pp. 407–410, 1996.

[6] F. E. Perrier, G. Petiau, G. Clerc et al., "A one-year systematic study of electrodes for long period measurements of the electric field in geophysical environments," *Journal of Geomagnetism and Geoelectricity*, vol. 49, pp. 1677–1696, 1997.

[7] M. Aubert and G. Kieffer, "Underground water circulation within volcanic structures of mount Etna southern flank. Results of PS meausrements," *Comptes Rendus de l'Academie des Sciences*, vol. 296, pp. 1003–1006, 1984.

[8] M. Aubert and Q. Y. Atangana, "Self-potential method in hydrogeological exploration of volcanic areas," *Ground Water*, vol. 34, no. 6, pp. 1010–1016, 1996.

[9] J.-F. Lénat, D. Fitterman, D. B. Jackson, and P. Labazuy, "Geoelectrical structure of the central zone of Piton de la fournaise volcano (Reunion)," *Bull Volcanol*, vol. 62, no. 2, pp. 75–89, 2000.

[10] A. Finizola, F. Sortino, J.-F. Lénat, and M. Valenza, "Fluid circulation at Stromboli volcano (Aeolian Islands, Italy) from self-potential and CO_2 surveys," *Journal of Volcanology and Geothermal Research*, vol. 116, no. 1-2, pp. 1–18, 2002.

[11] A. Finizola, F. Sortino, J.-F. Lénat, M. Aubert, M. Ripepe, and M. Valenza, "The summit hydrothermal system of Stromboli. new insights from self-potential, temperature, CO_2 and fumarolic fluid measurements, with structural and monitoring implications," *Bulletin of Volcanology*, vol. 65, no. 7, pp. 486–504, 2003.

[12] A. Finizola, J. F. Lénat, O. Macedo, D. Ramos, J. C. Thouret, and F. Sortino, "Fluid circulation and structural discontinuities inside Misti volcano (Peru) inferred from self-potential measurements," *Journal of Volcanology and Geothermal Research*, vol. 135, no. 4, pp. 343–360, 2004.

[13] H. Hase, T. Hashimoto, S. Sakanaka, W. Kanda, and Y. Tanaka, "Hydrothermal system beneath Aso volcano as inferred from self-potential mapping and resistivity structure," *Journal of Volcanology and Geothermal Research*, vol. 143, no. 4, pp. 259–277, 2005.

[14] G. Saracco, P. Labazuy, and F. Moreau, "Localization of self-potential sources in volcano-electric effect with complex continuous wavelet transform and electrical tomography methods for an active volcano," *Geophysical Research Letters*, vol. 31, no. 12, Article ID L12610, 5 pages, 2004.

[15] G. Mauri, G. Williams-Jones, and G. Saracco, "Depth determinations of shallow hydrothermal systems by self-potential and multi-scale wavelet tomography," *Journal of Volcanology*

and Geothermal Research, vol. 191, no. 3-4, pp. 233–244, 2010.

[16] T. Ishido, T. Kikuchi, N. Matsushima et al., "Repeated self-potential profiling of Izu-Oshima volcano, Japan," *Journal of Geomagnetism and Geoelectricity*, vol. 49, pp. 1267–1278, 1997.

[17] T. Ishido, "Electrokinetic mechanisms for the "W"-shaped self-potential profile on volcanoes," *Geophysical Research Letters*, vol. 31, no. 15, Article ID L15616, 5 pages, 2004.

[18] S. Onizawa, N. Matsushima, T. Ishido, H. Hase, S. Takakura, and Y. Nishi, "Self-potential distribution on active volcano controlled by three-dimensional resistivity structure in Izu-Oshima, Japan," *Geophysical Journal International*, vol. 178, no. 2, pp. 1164–1181, 2009.

[19] R. Antoine, D. Baratoux, M. Rabinowicz et al., "Thermal infrared image analysis of a quiescent cone on Piton de la Fournaise volcano: Evidence of convective air flow within an unconsolidated soil," *Journal of Volcanology and Geothermal Research*, vol. 183, no. 3-4, pp. 228–244, 2009.

[20] F. Perrier and P. Morat, "Characterization of electrical daily variations induced by capillary flow in the non-saturated zone," *Pure and Applied Geophysics*, vol. 157, no. 5, pp. 785–810, 2000.

[21] X. Guichet, L. Jouniaux, and J.-P. Pozzi, "Streaming potential of a sand column in partial saturation conditions," *Journal of Geophysical Research B*, vol. 108, article 2141, 12 pages, 2003.

[22] A. Revil, N. Linde, A. Cerepi, D. Jougnot, S. Matthäi, and S. Finsterle, "Electrokinetic coupling in unsaturated porous media," *Journal of Colloid and Interface Science*, vol. 313, no. 1, pp. 315–327, 2007.

[23] V. Allègre, L. Jouniaux, F. Lehmann, and P. Sailhac, "Streaming potential dependence on water-content in Fontainebleau sand," *Geophysical Journal International*, vol. 182, no. 3, pp. 1248–1266, 2010.

[24] V. Allègre, L. Jouniaux, F. Lehmann, and P. Sailhac, "Streaming potential dependence on water-content in fontainebleau sand," *Geophysical Journal International*, vol. 186, no. 1, pp. 115–117, 2011, Reply to the comment by A. Revil and N. Linde.

[25] H. Mizutani, T. Ishido, T. Yokokura, and S. Ohnishi, "Electrokinetic phenomena associated with earthquakes," *Geophysical Research Letters*, vol. 3, pp. 365–368, 1976.

[26] R. F. Corwin and H. F. Morrison, "Self potential variations preceding earthquakes in central california," *Geophysical Research Letters*, vol. 4, no. 4, pp. 171–174, 1977.

[27] A. Nur, "Dilatancy, pore fluids, and premonitory variations of ts/tp travel times," *Bulletin of the Seismological society of America*, vol. 62, pp. 1217–1222, 1972.

[28] C. H. Scholz, L. R. Sykes, and Y. P. Aggarwal, "Earthquake prediction: a physical basis," *Science*, vol. 181, no. 4102, pp. 803–810, 1973.

[29] H. Murakami, H. Mizutani, and S. Nabetani, "Self-potential anomalies associated with an active fault," *Journal of Geomagnetism & Geoelectricity*, vol. 36, no. 9, pp. 351–376, 1984.

[30] I. Dobrovolsky, N. Gershenzon, and M. Gokhberg, "Theory of electrokinetic effects occurring at the final stage in the preparation of a tectonic earthquake," *Physics of the Earth and Planetary Interiors*, vol. 57, no. 1-2, pp. 144–156, 1989.

[31] P. Bernard, "Plausibility of long distance electrotelluric precursors to earthquakes," *Journal of Geophysical Research*, vol. 97, pp. 17531–17546, 1992.

[32] L. Jouniaux and J. P. Pozzi, "Streaming potential and permeability of saturated sandstones under triaxial stress: consequences for electrotelluric anomalies prior to earthquakes," *Journal of Geophysical Research*, vol. 100, no. 6, pp. 10197–10209, 1995.

[33] B. Lorne, F. Perrier, and J. P. Avouac, "Streaming potential measurements 2. Relationship between electrical and hydraulic flow patterns from rock samples during deformation," *Journal of Geophysical Research B*, vol. 104, no. 8, pp. 17879–17896, 1999.

[34] M. Fenoglio, M. Johnston, and J. Byerlee, "Magnetic and electric fields associated with changes in high pore pressure in fault zones: application to the loma prieta ULF emissions," *Journal of Geophysical Research*, vol. 100, pp. 12951–12958, 1995.

[35] J. Miyakoshi, "Anomalous time variation of the sel-potential in the fractured zone of an active fault preceding the earthquake occurence," *Journal of Geomagnetism and Geoelectricity*, vol. 38, pp. 1015–1030, 1986.

[36] C. W. Hunt and M. H. Worthington, "Borehole electrokinetic responses in fracture dominated hydraulically conductive zones," *Geophysical Research Letters*, vol. 27, no. 9, pp. 1315–1318, 2000.

[37] J. Moore and S. Glaser, "Self-potential observations during hydraulic fracturing," *Journal of Geophysical Research*, vol. 112, no. 2, Article ID B02204, 2007.

[38] N. Cuevas, J. Rector, J. Moore, and S. Glaser, "Electrokinetic coupling in hydraulic fracture propagation," *SEG Technical Program Expanded Abstracts*, vol. 28, no. 1, pp. 1721–1725, 2009.

[39] T. Ishido, H. Mizutani, and K. Baba, "Streaming potential observations, using geothermal wells and in situ electrokinetic coupling coefficients under high temperature," *Tectonophysics*, vol. 91, no. 1-2, pp. 89–104, 1983.

[40] G. Marquis, M. Darnet, P. Sailhac, A. K. Singh, and A. Gérard, "Surface electric variations induced by deep hydraulic stimulation: an example from the Soultz HDR site," *Geophysical Research Letters*, vol. 29, article 1662, 4 pages, 2002.

[41] M. Darnet and G. Marquis, "Modelling streaming potential (SP) signals induced by water movement in the vadose zone," *Journal of Hydrology*, vol. 285, no. 1–4, pp. 114–124, 2004.

[42] A. Maineult, Y. Bernabé, and P. Ackerer, "Detection of advected, recating redox fronts from self-potential measurements," *Journal of Contaminant Hydrology*, vol. 86, pp. 32–52, 2006.

[43] A. Maineult, M. Darnet, and G. Marquis, "Correction to on the origins of self-potential (SP) anomalies induced by water injections into geothermal reservoirs," *Geophysical Research Letters*, vol. 33, Article ID L20319, 2006.

[44] A. Maineult, L. Jouniaux, and Y. Bernabé, "Influence of the mineralogical composition on the self-potential response to advection of kcl concentration fronts through sand," *Geophysical Research Letters*, vol. 33, Article ID L24311, 2006.

[45] M. Darnet, G. Marquis, and P. Sailhac, "Hydraulic stimulation of geothermal reservoirs: fluid flow, electric potential and microseismicity relationships," *Geophysical Journal International*, vol. 166, no. 1, pp. 438–444, 2006.

[46] A. Maineult, E. Strobach, J. Renner et al., "Self-potential signals induced by periodic pumping," *Journal of Geophysical Research*, vol. 113, Article ID B01203, 12 pages, 2008.

[47] C. Doussan, L. Jouniaux, and J.-L. Thony, "Variations of self-potential and unsaturated water flow with time in sandy loam and clay loam soils," *Journal of Hydrology*, vol. 267, no. 3-4, pp. 173–185, 2002.

[48] P. Sailhac and G. Marquis, "Analytic potentials for the forward and inverse modeling of SP anomalies caused by

subsurface fluid flow," *Geophysical Research Letters*, vol. 28, no. 9, pp. 1851–1854, 2001.

[49] M. Darnet, G. Marquis, and P. Sailhac, "Estimating aquifer hydraulic properties from the inversion of surface streaming potential (SP) anomalies," *Geophysical Research Letters*, vol. 30, article 1679, 2003.

[50] F. Perrier, M. Trique, B. Lorne, J.-P. Avouac, S. Hautot, and P. Tarits, "Electric potential variations associated with yearly lake level variations," *Geophysical Research Letters*, vol. 25, no. 10, pp. 1955–1958, 1998.

[51] L. Jouniaux, J.-P. Pozzi, and J. Berthier, "Detection of fluid flow variations at the Nankai trough by electric and magnetic measurements in boreholes or at the seafloor," *Journal of Geophysical Research B*, vol. 104, no. 12, pp. 29293–29309, 1999.

[52] J. H. Saunders, M. D. Jackson, and C. C. Pain, "Fluid flow monitoring in oilfields using downhole measurements of electrokinetic potential," *Geophysics*, vol. 73, no. 5, pp. E165–E180, 2008.

[53] D. Fitterman, "Electrokinetic and magnetic anomalies associated with dilatant regions in a layered earth," *Journal of Geophysical Research*, vol. 83, pp. 5923–5928, 1978.

[54] C. Fournier, *Méthodes géoélectriques appliquées à l'hydrogéologie en région volcanique; Développement de la méthode des potentiels spontanés en hydrogéologie*, Ph.D. thesis, University of Clermont-Ferrand, 1983.

[55] W. Sill, "Self-potential modeling from primary flows," *Geophysics*, vol. 48, no. 1, pp. 76–86, 1983.

[56] C. Fournier, "Spontaneous potentials and resistivity surveys applied to hydrogeology in a volcanic area: case history of the Chaine des Puys (France)," *Geophysical Prospecting*, vol. 37, pp. 647–668, 1988.

[57] T. Ishido and J. Pritchett, "Numerical simulation of electrokinetic potentials associated with subsurface fluid flow," *Journal of Geophysical Research B*, vol. 104, no. 7, pp. 15247–15259, 1999.

[58] M. Sheffer and D. Oldenburg, "Three-dimensional modelling of streaming potential," *Geophysical Journal International*, vol. 169, no. 3, pp. 839–848, 2007.

[59] D. Gilbert and M. Pessel, "Identification of sources potential fields with the continuous wavelet transform: application to self-potential profiles," *Geophysical Research Letters*, vol. 28, no. 9, pp. 1863–1866, 2001.

[60] P. Sailhac, M. Darnet, and G. Marquis, "Electrical streaming potential measured at the ground surface: forward modeling and inversion issues for monitoring infiltration and characterizing the vadose zone," *Vadose Zone Journal*, vol. 3, pp. 1200–1206, 2004.

[61] D. Gibert and P. Sailhac, "Comment on: self-potential signals associated with preferential grounwater flow pathways in sinkholes," *Journal of Geophysical Research*, vol. 113, Article ID B03210, 2008, by A. Jardani, J. P. Dupont, A. Revil.

[62] B. Minsley, J. Sogade, and F. Morgan, "Three-dimensional modelling source inversion of self-potential data," *Journal of Geophysical Research*, vol. 112, Article ID B02202, 13 pages, 2007.

[63] V. Naudet, J. Fernandez-Martinez, E. Garcia-Gonzalo, and J. Fernandez-Alvarez, "Estimation of water table from self-potential data using particle swarm optimization (pso)," *SEG Expanded Abstracts*, vol. 27, pp. 1203–1207, 2008.

[64] H. El-Kaliouby and M. Al-Garni, "Inversion of self-potential anomalies caused by 2D inclined sheets using neural networks," *Journal of Geophysics and Engineering*, vol. 6, no. 1, pp. 29–34, 2009.

[65] J. Fernandez-Martinez, E. Garcia-Gonzalo, and V. Naudet, "Particle swarm optimization applied to solving and appraising the streaming-potential inverse problem," *Geophysics*, vol. 75, no. 4, pp. WA3–WA15, 2010.

[66] P. Pezard, S. Gautier, T. L. Borgne, B. Legros, and J. L. Deltombe, "MuSET: a multiparameter and high precision sensor for downhole spontaneous electrical potential measurements," *Comptes Rendus Geoscience*, vol. 341, no. 10-11, pp. 957–964, 2009.

[67] S. Li, D. Pengra, and P. Wong, "Onsager's reciprocal relation and the hydraulic permeability of porous media," *Physical Review E*, vol. 51, no. 6, pp. 5748–5751, 1995.

[68] P. W. J. Glover, I. I. Zadjali, and K. A. Frew, "Permeability prediction from MICP and NMR data using an electrokinetic approach," *Geophysics*, vol. 71, no. 4, pp. F49–F60, 2006.

[69] H. Murakami, T. Hashimoto, N. Oshiman, S. Yamaguchi, Y. Honkura, and N. Sumitomo, "Electrokinetic phenomena associated with a water injection experiment at the Nojima fault on Awaji Island, Japan," *The Island Arc*, vol. 10, no. 3-4, pp. 244–251, 2001.

[70] K. E. Butler and R. D. Russell, "Subtraction of powerline harmonics from geophysical records," *Geophysics*, vol. 58, no. 6, pp. 898–903, 1993.

[71] K. E. Butler and R. D. Russell, "Cancellation of multiple harmonic noise series in geophysical records," *Geophysics*, vol. 68, no. 3, pp. 1083–1090, 2003.

[72] D. Beamish, "Characteristics of near surface electrokinetic coupling," *Geophysical Journal International*, vol. 137, no. 1, pp. 231–242, 1999.

[73] A. Thompson, S. Hornbostel, J. Burns et al., "Field tests of electroseismic hydrocarbon detection," *SEG Technical Program Expanded Abstracts*, vol. 24, p. 565, 2005.

[74] J. C. Dupuis, K. E. Butler, and A. W. Kepic, "Seismoelectric imaging of the vadose zone of a sand aquifer," *Geophysics*, vol. 72, no. 6, pp. A81–A85, 2007.

[75] M. H. P. Strahser, W. Rabbel, and F. Schildknecht, "Polarisation and slowness of seismoelectric signals: a case study," *Near Surface Geophysics*, vol. 5, no. 2, pp. 97–114, 2007.

[76] S. S. Haines, A. Guitton, and B. Biondi, "Seismoelectric data processing for surface surveys of shallow targets," *Geophysics*, vol. 72, no. 2, pp. G1–G8, 2007.

[77] S. Haines, *Seismoelectric imaging of shallow targets*, Ph.D. dissertation, Stanford University, 2004.

[78] A. W. Adamson, *Physical Chemistry of Surfaces*, John Wiley & Sons, New York, NY, USA, 1976.

[79] J. A. Davis, R. O. James, and J. Leckie, "Surface ionization and complexation at the oxide/water interface. I. Computation of electrical double layer properties in simple electrolytes," *Journal of Colloid And Interface Science*, vol. 63, no. 3, pp. 480–499, 1978.

[80] R. Hunter, *Zeta Potential in Colloid Science: Principles and Applications*, Academic, New York, NY, USA, 1981.

[81] P. Glover and M. Jackson, "Borehole electrokinetics," *The Leading Edge*, vol. 29, no. 6, pp. 724–728, 2010.

[82] S. Pride, "Governing equations for the coupled electromagnetics and acoustics of porous media," *Physical Review B*, vol. 50, no. 21, pp. 15678–15696, 1994.

[83] J. Davis and D. Kent, "Surface complexation modeling in aqueous geochemistry," in *Mineral Water Interface Geochemistry*, M. F. Hochella and A. F. White, Eds., Mineralogical Society of America, 1990.

[84] G. Sposito, *The Chemistry of Soils*, Oxford University, Oxford, UK, 1989.

[85] G. Parks, "The isoelectric points of solid oxides, solid hydroxides, and aqueous hydroxo complex systems," *Chemical Reviews*, vol. 65, no. 2, pp. 177–198, 1965.

[86] B. Lorne, F. Perrier, and J.-P. Avouac, "Streaming potential measurements: 1. Properties of the electrical double layer from crushed rock samples," *Journal of Geophysical Research B*, vol. 104, no. 8, pp. 17857–17877, 1999.

[87] P. Van Cappellen, L. Charlet, W. Stumm, and P. Wersin, "A surface complexation model of the carbonate mineral-aqueous solution interface," *Geochimica et Cosmochimica Acta*, vol. 57, no. 15, pp. 3505–3518, 1993.

[88] X. Guichet, L. Jouniaux, and N. Catel, "Modification of streaming potential by precipitation of calcite in a sand-water system: laboratory measurements in the pH range from 4 to 12," *Geophysical Journal International*, vol. 166, no. 1, pp. 445–460, 2006.

[89] L. Onsager, "Reciprocal relations in irreversible processes. I," *Physical Review*, vol. 37, no. 4, pp. 405–426, 1931.

[90] D. Miller, "Thermodynamics of irreversible processes: the experimental verification of the onsager reciprocal relations," *Chemical Reviews*, vol. 60, no. 1, pp. 15–37, 1960.

[91] J. Auriault and T. Strzelecki, "On the electro-osmotic flow in a saturated porous medium," *International Journal of Engineering Science*, vol. 19, no. 7, pp. 915–928, 1981.

[92] K. Beddiar, Y. Berthaud, and A. Dupas, "Experimental verification of the onsager's reciprocal relations for electro-osmosis and electro-filtration phenomena on a saturated clay," *Comptes Rendus Mécanique*, vol. 330, no. 12, pp. 893–898, 2002.

[93] V. Allègre, F. Lehmann, P. Ackerer, L. Jouniaux, and P. Sailhac, "Modelling the streaming potential dependence on water content during drainage: 1. A 1D modelling of SP using finite element method," *Geophysical Journal International*. In press.

[94] L. Jouniaux, M.-L. Bernard, M. Zamora, and J.-P. Pozzi, "Streaming potential in volcanic rocks from Mount Peleé," *Journal of Geophysical Research B*, vol. 105, no. 4, pp. 8391–8401, 2000.

[95] S. S. Dukhin and B. V. Derjaguin, *Surface and Colloid Science*, John Wiley & Sons, New York, NY, USA, 1974, Edited by E. Matijevic.

[96] T. Ishido and H. Muzutani, "Experimental and theoretical basis of electrokinetic phenomena in rock-water systems and its applications to geophysics," *Journal of Geophysical Research*, vol. 86, no. 3, pp. 1763–1775, 1981.

[97] L. Jouniaux and J.-P. Pozzi, "Permeability dependence of streaming potential in rocks for various fluid conductivities," *Geophysical Research Letters*, vol. 22, no. 4, pp. 485–488, 1995.

[98] M. Z. Jaafar, J. Vinogradov, and M. D. Jackson, "Measurement of streaming potential coupling coefficient in sandstones saturated with high salinity NaCl brine," *Geophysical Research Letters*, vol. 36, no. 21, Article ID L21306, 2009.

[99] J. Vinogradov, M. Jaafar, and M. D. Jackson, "Measurement of streaming potential coupling coefficient in sandstones saturated with natural and artificial brines at high salinity," *Journal of Geophysical Research B*, vol. 115, no. 12, Article ID B12204, 2010.

[100] M. Ahmad, "A laboratory study of streaming potentials," *Geophysical Prospecting*, vol. 12, no. 1, pp. 49–64, 1964.

[101] L. Jouniaux and J.-P. Pozzi, "Laboratory measurements anomalous 0.1–0.5 Hz streaming potential under geochemical changes: implications for electrotelluric precursors to earthquakes," *Journal of Geophysical Research B*, vol. 102, no. 7, pp. 15335–15343, 1997.

[102] D. B. Pengra, S. X. Li, and P.-Z. Wong, "Determination of rock properties by low-frequency AC electrokinetics," *Journal of Geophysical Research B*, vol. 104, no. 12, pp. 29485–29508, 1999.

[103] F. Perrier and T. Froidefond, "Electrical conductivity and streaming potential coefficient in a moderately alkaline lava series," *Earth and Planetary Science Letters*, vol. 210, no. 1-2, pp. 351–363, 2003.

[104] S. Pride and M. W. Haartsen, "Electroseismic wave properties," *Journal of the Acoustical Society of America*, vol. 100, no. 3, pp. 1301–1315, 1996.

[105] B. White and M. Zhou, "Electroseismic prospecting in layered media," *SIAM Journal on Applied Mathematics*, vol. 67, no. 1, pp. 69–98, 2006.

[106] D. Smeulders, R. Eggels, and M. van Dongen, "Dynamic permeability: reformulation of theory and new experimental and numerical data," *Journal of Fluid Mechanics*, vol. 245, pp. 211–227, 1992.

[107] P. M. Reppert, F. D. Morgan, D. P. Lesmes, and L. Jouniaux, "Frequency-dependent streaming potentials," *Journal of Colloid and Interface Science*, vol. 234, no. 1, pp. 194–203, 2001.

[108] D. L. Johnson, J. Koplik, and R. Dashen, "Theory of dynamic permeability in fluid saturated porous media," *Journal of Fluid Mechanics*, vol. 176, pp. 379–402, 1987.

[109] R. G. Packard, "Streaming potentials across glass capillaries for sinusoidal pressure," *The Journal of Chemical Physics*, vol. 21, pp. 303–307, 1953.

[110] C. E. Cooke, "Study of electrokinetic effects using sinusoidal pressure and voltage," *The Journal of Chemical Physics*, vol. 23, no. 12, pp. 2299–2303, 1955.

[111] J. Groves and A. Sears, "Alternating streaming current measurements," *Journal of Colloid And Interface Science*, vol. 53, no. 1, pp. 83–89, 1975.

[112] A. Sears and J. Groves, "The use of oscillating laminar flow streaming potential measurements to determine the zeta potential of a capillary surface," *Journal of Colloid And Interface Science*, vol. 65, no. 3, pp. 479–482, 1978.

[113] R. Chandler, "Transient streaming potential measurements on fluid-saturated porous structures: an experimental verification of Biot's slow wave in the quasi-static limit," *Journal of the Acoustical Society of America*, vol. 70, no. 1, pp. 116–121, 1981.

[114] F. Schoemaker, D. Smeulders, and E. Slob, "Simultaneous determination of dynamic permeability and streaming potential," *SEG Technical Program Expanded Abstracts*, vol. 26, no. 1, pp. 1555–1559, 2007.

[115] F. C. Schoemaker, D. M. J. Smeulders, and E. C. Slob, "Electrokinetic effect: theory and measurement," *SEG Technical Program Expanded Abstracts*, vol. 27, no. 1, pp. 1645–1649, 2008.

[116] E. Tardif, P. Glover, and J. Ruel, "Frequency-dependent streaming potential of Ottawa sand," *Journal of Geophysical Research B*, vol. 116, no. 4, Article ID B04206, 2011.

[117] M. W. Haartsen and S. R. Pride, "Electroseismic waves from point sources in layered media," *Journal of Geophysical Research B*, vol. 102, no. b11, pp. 24745–24769, 1997.

[118] M. W. Haartsen, W. Dong, and M. N. Toksöz, "Dynamic streaming currents from seismic point sources in homogeneous poroelastic media," *Geophysical Journal International*, vol. 132, no. 2, pp. 256–274, 1998.

[119] S. Garambois and M. Dietrich, "Seismoelectric wave conversions in porous media: field measurements and transfer function analysis," *Geophysics*, vol. 66, no. 5, pp. 1417–1430, 2001.

[120] S. Garambois and M. Dietrich, "Full waveform numerical simulations of seismoelectromagnetic wave conversions in fluid-saturated stratified porous media," *Journal of Geophysical Research B*, vol. 107, no. 7, Article ID 2148, 2002.

[121] C. Pain, J. H. Saunders, M. H. Worthington et al., "A mixed finite-element method for solving the poroelastic Biot equations with electrokinetic coupling," *Geophysical Journal International*, vol. 160, no. 2, pp. 592–608, 2005.

[122] M. Schakel and D. Smeulders, "Seismoelectric reflection and transmission at a fluid/porous-medium interface," *Journal of the Acoustical Society of America*, vol. 127, no. 1, pp. 13–21, 2010.

[123] Y. Gao and H. Hu, "Seismoelectromagnetic waves radiated by a double couple source in a saturated porous medium," *Geophysical Journal International*, vol. 181, no. 2, pp. 873–896, 2010.

[124] Z. Zhu, M. W. Haartsen, and M. N. Toksöz, "Experimental studies of electrokinetic conversions in fluid-saturated borehole models," *Geophysics*, vol. 64, no. 5, pp. 1349–1356, 1999.

[125] B. Chen and Y. Mu, "Experimental studies of seismoelectric effects in fluid-saturated porous media," *Journal of Geophysics and Engineering*, vol. 2, no. 3, pp. 222–230, 2005.

[126] C. Bordes, L. Jouniaux, M. Dietrich, J.-P. Pozzi, and S. Garambois, "First laboratory measurements of seismomagnetic conversions in fluid-filled fontainebleau sand," *Geophysical Research Letters*, vol. 33, Article ID L01302, 5 pages, 2006.

[127] G. I. Block and J. G. Harris, "Conductivity dependence of seismoelectric wave phenomena in fluid-saturated sediments," *Journal of Geophysical Research B*, vol. 111, no. 1, Article ID B01304, 12 pages, 2006.

[128] C. Bordes, L. Jouniaux, S. Garambois, M. Dietrich, J.-P. Pozzi, and S. Gaffet, "Evidence of the theoretically predicted seismo-magnetic conversion," *Geophysical Journal International*, vol. 174, no. 2, pp. 489–504, 2008.

[129] M. Schakel, D. Smeulders, E. Slob, and H. Heller, "Seismoelectric interface response: experimental results and forward model," *Geophysics*, vol. 76, no. 4, pp. N29–N36, 2011.

[130] R. R. Thompson, "The seismic-electric effect," *Geophysics*, vol. 1, no. 3, pp. 327–335, 1936.

[131] S. T. Martner and N. R. Sparks, "The electroseismic effect," *Geophysics*, vol. 24, no. 2, pp. 297–308, 1959.

[132] L. T. Long and W. K. Rivers, "Field measurement of the electroseismic response," *Geophysics*, vol. 40, no. 2, pp. 233–245, 1975.

[133] M. Strahser, L. Jouniaux, P. Sailhac, P.-D. Matthey, and M. Zillmer, "Dependence of seismoelectric amplitudes on water-content," *Geophysical Journal International*, vol. 187, no. 3, pp. 1378–1392, 2011.

[134] J. C. Dupuis, K. E. Butler, A. W. Kepic, and B. D. Harris, "Anatomy of a seismoelectric conversion: measurements and conceptual modeling in boreholes penetrating a sandy aquifer," *Journal of Geophysical Research B*, vol. 114, Article ID B10306, 9 pages, 2009.

[135] S. S. Haines, S. R. Pride, S. L. Klemperer, and B. Biondi, "Seismoelectric imaging of shallow targets," *Geophysics*, vol. 72, no. 2, pp. G9–G20, 2007.

[136] J. C. Dupuis and K. E. Butler, "Vertical seismoelectric profiling in a borehole penetrating glaciofluvial sediments," *Geophysical Research Letters*, vol. 33, no. 16, Article ID L16301, 2006.

[137] A. Zohdy, L. Anderson, and L. Muffler, "Resistivity, self-potential, and induced polarization surveys of a vapor dominated geothermal system," *Geophysics*, vol. 38, no. 6, pp. 1130–1144, 1973.

[138] L. Anderson and G. Johnson, "Application of the self-Potential method to geothermal exploration in Long Valley, California," *Journal of Geophysical Research*, vol. 81, no. 8, pp. 1527–1532, 1976.

[139] R. Corwin and D. Hoover, "The self-potential method in geothermal exploration," *Geophysics*, vol. 44, no. 2, pp. 226–245, 1979.

[140] B. Wurmstich and F. Morgan, "Modeling of streaming potential responses caused by oil well pumping," *Geophysics*, vol. 59, no. 1, pp. 46–56, 1994.

[141] M. Grant, I. Donaldson, and P. Bixley, *Geothermal Reservoir Engineering*, vol. 72, Academic press, 1982.

[142] T. Ishido, "Streaming potential associated with hydrothermal convection in the crust: a possible mechanism of self-potential anomalies in geothermal areas," *Journal of the Geothermal Research Society of Japan*, vol. 3, pp. 87–100, 1981.

[143] T. Ishido, T. Kikuchi, Y. Yano, M. Sugihara, and S. Nakao, "Hydrogeology inferred from the self-potential distribution, Kirishima geothermal field, Japan," *Geothermal Resources Council Transactions*, vol. 14, no. 2, pp. 916–926, 1990.

[144] M. Hochstein, I. Mayhew, and R. Villarosa, "Self-potential surveys of the Mokai and Rotokawa high temperature fields (NZ)," in *Proceedings of the 12th New Zealand Geothermal Workshop*, vol. 17, pp. 87–89, 1990.

[145] T. Ishido, T. Kikuchi, and M. Sugihara, "Mapping thermally driven upflows by the selfpotential method," in *Hydrogeological Regimes and Their Subsurface Thermal Effects*, vol. 47 of *Geophysical Monograph*, pp. 151–158, 1989.

[146] J. Zlotnicki and Y. Nishida, "Review on morphological insights of self-potential anomalies on volcanoes," *Surveys in Geophysics*, vol. 24, no. 4, pp. 291–338, 2003.

[147] P. Reppert and F. Morgan, "Temperature-dependent streaming potentials: 2. Laboratory," *Journal of Geophysical Research B*, vol. 108, no. 11, Article ID 2547, 13 pages, 2003.

[148] T. Tosha, N. Matsushima, and T. Ishido, "Zeta potential measured for an intact granite sample at temperatures to 200°C," *Geophysical Research Letters*, vol. 30, no. 6, Article ID 1295, 4 pages, 2003.

[149] T. Ishido and N. Matsushima, "Streaming potential measured for an intact rock sample at temperatures to 200°C," in *Proceedings of the 32nd Workshop on Geothermal Reservoir Engineering*, Stanford University, 2007.

[150] H. Hase, T. Ishido, S. Takakura, T. Hashimoto, K. Sato, and Y. Tanaka, "Zeta potential measurement of volcanic rocks from Aso caldera," *Geophysical Research Letters*, vol. 23, no. 30, Article ID 2210, 2003.

[151] K. Aizawa, M. Uyeshima, and K. Nogami, "Zeta potential estimation of volcanic rocks on 11 island arc-type volcanoes in Japan: implication for the generation of local self-potential anomalies," *Journal of Geophysical Research*, vol. 113, no. 2, Article ID B02201, 2008.

[152] P. Glover and N. Déry, "Streaming potential coupling coefficient of quartz glass bead packs: dependence on grain diameter, pore size, and pore throat radius," *Geophysics*, vol. 75, no. 6, pp. F225–F241, 2010.

[153] C. Zablocki, "Mapping thermal anomalies on an active volcano by the self-potential method, Kilauea, Hawaii," in *Proceedings of the 2nd U.N. Symposium on the Development and Use of Geothermal Resources*, vol. 2, pp. 1299–1309, San Francisco, Calif, USA, 1976.

[154] T. Hashimoto and Y. Tanaka, "A large self-potential anomaly on Unzen volcano, Shimabara Peninsula, Kyushu Island, Japan," *Geophysical Research Letters*, vol. 22, no. 3, pp. 191–194, 1995.

[155] Y. Nishida, N. Matsushima, A. Goto et al., "Self-potential studies in volcanic areas (3) Miyake-jima, Esan and Usu," *Journal of the Hokkaido University Series 7*, vol. 10, no. 1, pp. 63–77, 1996.

[156] Y. Sasai, J. Zlotnicki, Y. Nlshida et al., "Electromagnetic monitoring of Miyake-jima volcano, Izu-Bonin arc, Japan: A preliminary report," *Journal of Geomagnetism and Geoelectricity*, vol. 49, no. 11-12, pp. 1293–1316, 1997.

[157] S. Michel and J. Zlotnicki, "Self-potential and magnetic surveying of la Fournaise volcano (Reunion Island): correlations with faulting, fluid circulation, and eruption," *Journal of Geophysical Research B*, vol. 103, no. 8, pp. 17845–17857, 1998.

[158] K. Aizawa, "A large self-potential anomaly and its changes on the quiet Mt. Fuji, Japan," *Geophysical Research Letters*, vol. 31, no. 5, Article ID L05612, 4 pages, 2004.

[159] P. Bedrosian, M. Unsworth, and M. Johnston, "Hydrothermal circulation at mount St. Helens determined by self-potential measurements," *Journal of Volcanology and Geothermal Research*, vol. 160, no. 1-2, pp. 137–146, 2007.

[160] K. Aizawa, "Classification of self-potential anomalies on volcanoes and possible interpretations for their subsurface structure," *Journal of Volcanology and Geothermal Research*, vol. 175, no. 3, pp. 253–268, 2008.

[161] C. Fournier, "Spontaneous potentials and resistivity surveys applied to hydrogeology in a volcanic area: case history of the Chaine des Puys (Puy-de-Dome, France)," *Geophysical Prospecting*, vol. 37, no. 6, pp. 647–668, 1989.

[162] A. Revil, V. Naudet, J. Nouzaret, and M. Pessel, "Principles of electrography applied to self-potential electrokinetic sources and hydrogeological applications," *Water Resources Research*, vol. 39, no. 5, Article ID 1114, 15 pages, 2003.

[163] C. Zablocki, R. Tilling, D. Peterson, and R. Christiansen, "A deep research drill hole at the summit of an active volcano, kilauea, Hawaii," *Geophysical Research Letters*, vol. 1, no. 7, pp. 323–326, 1974.

[164] K. Aizawa, Y. Ogawa, and T. Ishido, "Groundwater flow and hydrothermal systems within volcanic edifices: delineation by electric self-potential and magnetotellurics," *Journal of Geophysical Research*, vol. 114, no. 1, Article ID B01208, 2009.

[165] T. Ishido, *Volcano Monitoring Using Self-Potential Technique*, EGU General Assembly, Vienna, Austria, 2006, Abstract EGU06–A–00975.

[166] T. Ishido, *Self-Potential Changes Caused by Magma Ascent and Degassing*, AGU Fall Meeting, San Francisco, Calif, USA, 2009, Abstract V33F–03.

[167] B. Nourbehecht, *Irreversible thermodynamic effects in inhomogeneous media and their applications in certain geoelectric problems*, Ph.D. thesis, MIT Press, Cambridge, Mass, USA, 1963.

[168] D. Fitterman, "Correction to theory of electrokinetic-magnetic anomalies in a fault halfspace," *Journal of Geophysical Research*, vol. 86, pp. 9585–9588, 1981.

[169] T. Ishido, "Self-potential generation by subsurface water flow through electrokinetic coupling," in *Detection of Subsurface Flow Phenomena, Lecture Notes in Earth Sciences*, vol. 27, pp. 121–131, 1989.

[170] K. Yasukawa, T. Ishido, and I. Suzuki, "Geothermal reservoir monitoring by continuous self-potential measurements, Mori geothermal field, Japan," *Geothermics*, vol. 34, no. 5, pp. 551–567, 2005.

[171] T. Tosha, T. Ishido, N. Matsushima, and Y. Nishi, "Self-potential variation at the Yanaizu-Nishiyama geothermal field and its interpretation by the numerical simulation," in *Proceedings of the World Geothermal Congress*, vol. 3, pp. 1871–1876, Beppu-Morioka, Japan, 2000.

[172] Y. Nishi and T. Ishido, "Self-potential measurements for reservoir monitoring at the Okuaizu geothermal field," *Journal of the Geothermal Research Society of Japan*. In press.

[173] N. Matsushima, T. Kikuchi, T. Tosha et al., "Repeat SP measurements at the Sumikawa geothermal field, Japan," in *Proceedings of the World Geothermal Congress*, pp. 2725–2730, Beppu-Morioka, Japan, 2000.

[174] T. Ishido, *Changes in Self-Potential Caused by Redox Reaction*, SGEPPS, Sendai, Japan, 2008, Abstract A003–07.

[175] T. Ishido and J. Pritchett, "Prediction of magnetic field changes induced by geothermal fluid production and reinjection," *Geothermal Resources Council Transactions*, vol. 25, pp. 645–649, 2001.

[176] H. Mizutani and T. Ishido, "A new interpretation of magnetic field variation associated with the Matsushiro earthquakes," *Journal of Geomagnetism and Geoelectricity*, vol. 28, pp. 179–188, 1976.

[177] J. Zlotnicki and J. L. Mouel, "Possible electrokinetic origin of large magnetic variations at La Fournaise volcano," *Nature*, vol. 343, no. 6259, pp. 633–636, 1990.

[178] Y. Nishi, T. Ishido, M. Sugihara et al., "Reservoir monitoring in the Okuaizu geothermal field using multi-geophysical survey techniques," in *Proceedings of the World Geothermal Congress*, Antalya, Turkey, 2005.

[179] T. Ishido, K. Goko, T. Tosha, M. Adachi, J. Ishizaki, and Y. Nishi, "Reservoir monitoring using multi-geophysical survey techniques," *Geothermal Resources Council Transactions*, vol. 27, pp. 827–831, 2003.

[180] T. Ishido, K. Goko, M. Adachi et al., "System integration of various geophysical measurements for reservoir monitoring," in *Proceedings of the World Geothermal Congress*, Antalya, Turkey, April 2005.